Using Satellite Ground Operations Training To Develop An Algorithm Using Satellite Sea Surface Temperatures from the CERSER Ground Station to predict NOAA North Carolina Coastal Sea Buoy Temperatures

Ignatius Kweku Williams
Oceanography
University of Ghana
Accra, Ghana
idoublegy@gmail.com

Rockson Ashitey
Armaah Oceanography
University of Ghana
Accra, Ghana
armaahr@gmail.com

Je'aime Powell
Applied Mathematics
Elizabeth City State University
Elizabeth City, USA
jeaime.powell@cerser.ecsu.edu

Kuchumbi Hayden
Computer Science
Elizabeth City State University
Elizabeth City, USA
klhayden@mail.ecsu.edu

***Abstract*—Elizabeth City State University currently operates a TeraScan Grounding station capable of receiving and processing imagery data collected by satellites managed by the National Oceanic and Atmospheric Administration (NOAA). The imagery received in the Infrared spectrum both measures sea surface temperatures and cloud cover for the eastern coast of North Carolina. Once the data sets were collected, they were statistically analyzed using the analysis of variance methodology and regression. Strong correlations were observed during the AVHRR-Buoy comparison for two of the three areas under the study. The NOAA-16 AVHRR SST emerged as the most consistent with the insitu data from the ORIN7 Buoy. This was due to its high coefficient of determination. TeraScan training received during the period also contributed knowledge on the processing of raw data to suit specific areas of interest. The processed data could then be exported to third party software such as ENVI and Google Earth while maintaining the specific data of interest.**

Keywords-sattelite; sea surface temperature; buoys; image processing

I. INTRODUCTION

Temperature is an important environmental feature as its variation influences many other environmental activities such as evaporation. This study focuses mainly on sea surface temperature measurements that are collected by NOAA satellites (15,16,18,19) and three NOAA buoys (DKN7, ORIN7, HCGN7) located off the North Carolina coast. The temperature measurements used were obtained from satellite imagery and buoy data collected between the 22nd of April and 14th of June in the year 2011. Though many images were collected by the satellites within the dates stated, only 101 images where used due to the absence or presence of cloud cover over the regions of interest. This study aimed at developing an algorithm using the Satellite Sea Surface Temperatures (SST) and the buoy temperatures to model the variation between the measurements. Prior to the creation of the model, the variance between the sensors was statistically tested to determine if the differences were significant within a 95% level of confidence. The regression model was considered acceptable if a coefficient of determination of at least 50% was found.

II. LITERATURE REVIEW

A. Remote Sensing

Remote sensing is the measurement of object properties on earth's surface using data acquired from sensors mounted on platforms such as aircraft and satellites. It attempts to measure an object at a distance rather than insitu. Remote sensing systems deployed on satellites provide a repetitive and consistent view of the earth facilitating the ability to monitor the earth system and the effects of human activities on earth [1]. Remote sensing systems,

which measure naturally available energy, are called passive sensors. An example of this can only take place when the sun is illuminating the earth. There is no reflected energy available from the sun at night. Energy that is naturally emitted can be detected day and night provided that the amount of energy is large enough to be recorded [2]. Remote sensing systems, which provide their own source of energy for illumination, are known as active sensors. These sensors have the advantage of obtaining data any time of day or season. Synthetic Aperture Radar (SAR) is an example of an active sensor in the microwave spectrum [3].

B. Ground-Truthing

For the purpose of verification on remotely sensed data, Ground-Truthing is a necessary step in remote sensing activities. This mainly involves the collection of information from the remote sensed location that is especially important to relate image data to real features and materials on the ground. Ground-truth data enable calibration of remote sensing data and aids the interpretation and analysis of what is being sensed. Ground-Truthing is normally done on siteby performing surface observations and measurements of various properties of the ground resolution cells that are being studied on the remotely sensed digital image. Ground-Truthing is performed mainly to obtain relevant data and information that are helpful in the remotely sensed scene, to verify whether the data collected or identified is true or actually correct and to provide control measurements from targets of known identities [4].

C. Ground Stations

Ground Stations are specialized terrestrial stations designed to receive data products from orbiting satellites and transmitting sensors. Most Ground Stations are suited for twenty-four (24) hour weather and environmental monitoring anywhere on the globe. They continuously receive, process, archive and distribute data from every geosynchronous direct-readout satellite. Applications of these ground station datasets cover meteorology, oceanography, environmental studies and disaster management [5]. TeraScan low-resolution L- and S-band ground systems are the complete acquisition and data processing solutions for every major polar-orbiting low-resolution satellite [5]. Data received originate from multiple platforms such as Geostationary Operational Environmental Satellites (GOES), Meteosat, Meteosat Second Generation (MSG), Fengyun (FY series), National Oceanic and Atmospheric Administration (NOAA), Defense Meteorological Satellite Program (DMSP), Sea-viewing Wide Field-of-view Sensor (SeaWiFS), Metop, Aqua, Terra and more. TeraScan can also generate products that are a mixture of data from different satellites. The types of data that TeraScan can receive and process are listed in Table 1 Satellite Data that TeraScan Can Receive and Process.

Table 1 Satellite Data that TeraScan Can Receive and Process [6]

X-Band Data from Polar-Orbiting Satellites	L-/S-Band Data from Polar-Orbiting Satellites	L-Band Data from Geostationary Satellites	Other Data Sources
MODIS direct broadcast data from the Terra and Aqua EOS satellites (optional module)	AVHRR, TOVS, ATOVS, and DCS data from the NOAA TIROS-N satellites.	Imager and Sounder data from GOES.	MODIS EOS HDF from IMAPP
OCM data from Oceansat-1 (optional module).	SeaWiFS data from OrbView-2 (optional module).	HRI data from Meteosat (optional module).	NESDIS
SAR data (capture only) from Radarsat-1 and ERS-2.	OLS and Special Sensor data (SSM/I, SSM/T1, and SSM/T2) from the DMSP satellites.	Imager data from GMS and FY-2.	Archived data from SIO, Dundee, and ESA.
	MVISR data from FY-1C and FY-1D (optional module)	WEFAX data from GOES, Meteosat, and GMS.	

D. NOAA Sensors

The National Oceanographic and Atmospheric Administration ‘s (NOAA) environmental satellites provide data from space to monitor the Earth to analyze the coastal waters, relay life-saving emergency beacons, and track tropical storms and hurricanes. NOAA operates two types of satellite systems for the United States, geostationary satellites and polar-orbiting satellites. Geostationary satellites constantly monitor the Western

Hemisphere from ~22,240 miles above the Earth.Polar-orbiting satellites circle the Earth and provide global information from ~540 miles above the Earth [7]. Satellites enable the provision consistent, long-term observations, 24 hours a day, 7 days a week. They track fast breaking storms across "Tornado Alley" as well as tropical storms in the Atlantic and Pacific oceans. One measurementfrom satellites measure is the temperature of the ocean, which is a key indicator of climate change. Satellite information is also used to monitor coral reefs, harmful algal blooms, fires, and volcanic ash. Monitoring the Earth from space helps to promote understanding on how the Earth works and affects much of our daily lives [8]. NOAA's satellites provide other services beyond just imaging the Earth. Monitoring conditions in space and solar flares from the sun help us understand how conditions in space affect the Earth. Scientists also use a data collection system on the satellites to relay data from transmitters on the ground to researchers in the field. Historical data from these satellites, and other air-based and ground-based observation platforms, is archived for public use at NOAA's national data centers [9]. Currently, NOAA is operating five polar orbiters as seen in Table 2: NOAA Satellite Information.

Table 2: NOAA Satellite Information [10]

Satellite	Launched in	Repeat cycle	Orbit height	Orbit type
15-NOAA-K, morning	1998	11 days	833 km	Near polar-sun synchronous
16-NOAA-L, afternoon	2000	11 days	870 km	Near polar-sun synchronous
17-NOAA-M, morning	2002	11 days	833 km	Near polar-sun synchronous
18-NOAA-N	2005	11 days	870 km	Near polar-sun Afternoon
19-NOAA-N Prime	2009	11 days	870km	Near polar-sun synchronous

A new series of polar orbiters, with improved sensors, will begin with the launch of the **N**ational Polar-orbiting Operational Environmental Satellite System (NPOESS) **P**reparatory **P**roject (NPP) in May 2011 and NPOESS- C1 in September 2014. The most recent satellite, NOAA-19 is classified as the "operating" satellite while NOAA-15, NOAA-16, NOAA-17, NOAA-18 all continue transmitting as stand-by satellites. All the NOAA polar orbiting satellites make use of the following sensors [11].

- Advanced Very High Resolution Radiometers (AVHRR/3)
- Advanced microwave sounding unit- A (AMSU-A)
- Microwave Humidity Sounder (MHS)
- High Resolution Infrared Radiation Sounder (HIRS/4)
- Solar Backscatter Ultraviolet Spectral Radiometer (SBUV/2)

The newer NOAA-19 satellite uses the previous sensors in addition to the following sensors onboard [11];

- Space Environment Monitor (SEM/2)
- Search and Rescue (SAR) Repeater and processor
- Advance Data collection system (ADCS)

E. Advanced Very High Resolution Radiometer (AVHRR)

The Advanced Very High Resolution Radiometer is the primary sensor onboard the NOAA polar orbiting satellites. This instrument makes calibrated measurements of visible, near-infrared, and infrared radiation from the Earth and its atmosphere. These measurements are then interpreted as sea surface temperatures with algorithms applied to the image obtained through the sensor. Sea surface

temperatures are calculated based on readings from three of six channels used by the sensor. These are in shown in Table 3 : Spectral Bands of Infrared AVHRR channels.

Table 3 : Spectral Bands of Infrared AVHRR channels [12]

AVHRR Channel	Wavelength	EMR spectrum	Unit of measure
avhrr_ch3	3.55-3.93µm	near IR	temperature (°)
avhrr_ch4	10.3-11.3µm	thermal IR	temperature (°)
avhrr_ch5	11.5-12.5µm	thermal IR	temperature (°)

Equation 1

$$\mathbf{MCSST = 0.9367(T4) + 0.0864(Tf)\,(T4-T5) + 0.5979(T4-T5)(\sec(q) - 1.0) - 253.8050} \quad \mathbf{[13]}$$

NOAA satellites employ the algorithm in Equation 1 to calculate the Multi-Channeled Sea Surface Temperature (MCSST). Where T4 and T5 are the brightness temperatures for channel's 4 and 5 in degrees Kelvin, q is the zenith angle, and Tf is the analyzed field temperature. The coefficients used in the equation are based on calibration of the sensor. Most of the weight is given to channel 4. Channel 5 used as the water vapor correction. Additional weight is applied to the zenith angle of the satellite. Finally, the temperature is subtracted by 253.8050 in order to convert from degrees Kelvin (K°) to degrees Celsius (C°).

For Nonlinear Sea Surface Temperature the algorithm shown in **EQUATION 2** is applied.

Equation 2

$$\mathbf{NLSST = (A0 + A1*S)\,T4 + (B0 + B1*S + B2*T_{guess})\,*\,(T4-T5) + C0 + C1*S\ (2)} \quad \mathbf{[14]}$$

Where S = 1/cos(Sat. Zenith) – 1 and Tguess = Tclim (or AL0*T4 + CL0 + CL1*S) with all temperatures in Celsius. Also A, B0, B1, B2, C0 and C1 are constants, S = sec(satellite zenith angle), Tguess is a first guess SST, and T4 and T5 are the AVHRR channel 4 and 5 brightness temperatures. This gives the skin SST. A bias correction method is used to provide the bulk SST.

F. Sensor Spectrums

The electromagnetic radiation spectrum is very important in the principles and applications in the field of remote sensing. Currently, this knowledge has been incorporated in the sensors on board various satellites including the NOAA polar orbiting satellites. These make use of mainly the infrared, x-ray and microwave sectors of the spectrum. Examples of such applications include the Advanced Microwave sounding unit (AMSU) onboard all the NOAA polar orbiting satellites.

1) INFRARED

It is an electromagnetic radiation with a wavelength longer than that of visible light, measured from the nominal edge of visible red light at 0.7 micrometers, and extending conventionally to 300 micrometers [15]. William Herschel discovered it when he placed a thermometer just outside the red end of the color spectrum, it recorded a high temperature and so infrared is detected as heat. Examples are the heat radiated from fireplaces, campfires, sunlight and the ground [16].

2) MICROWAVES

Microwaves are electromagnetic waves with wavelengths ranging from as long as one meter to as short as one millimeter, or equivalently, with frequencies between 300 MHz (0.3 GHz) and 300 GHz [17]. Apparatus and techniques may be described qualitatively as "microwave" when the wavelengths of signals are roughly the same as the dimensions of the equipment, so that lumped element circuit theory is inaccurate. As a consequence, practical microwave technique tends to move away from the discrete resistors, capacitors, and inductors used with lower frequency radio waves. Instead, distributed circuit elements and transmission-line theory are more useful methods for design and analysis [18].

G. Image Processing Software

1) ILWIS

ILWIS or the Integrated Land and water Information system is a user-friendly GIS and remote sensing software package initiated in 1984 by the Dutch Government under an autonomous higher education institution [19]. It is one of the oldest GIS programs still in use [19]. As of 1st July 2007, ILWIS became an open source software and development of the software is now maintained by 52North, a consortium of open source developers [19]. Its capabilities include advanced modeling and spatial analysis, orthophoto and image referencing as well as a complete set of image processing tools [20]. These applications and capabilities make it ideal for academic users, educators, biologists, natural resources managers, and land-use planners. In current versions of ILWIS (ILWIS 3.7 OPEN), Plug-ins such as the GEONETCast Toolbox software has been incorporated [21, 22]. This enables easy access to various satellite and environmental products and/or resulting products. These in effect support subsequent and efficient geospatial processing [21].

2) ENVI

The Environment for Visualizing Images (ENVI) is a commercial image processing package. It is built upon IDL (Interactive Data Language) platform which allows customization and extension of ENVI as compared to other packages with similar processing capabilities [23]. ENVI boasts well-developed algorithms for hyperspectral and SAR images/data and hence is well suited for handling data from such sensors. These include Landsat, SPOT, Quickbird, ASTER, MODIS, AVHRR among others [24]. The software is also designed for the easy loading and display of polygons, points, contours and shapefiles [24]. ENVI thus provide advanced user-friendly tools to read, explore, analyze and share information extracted from al types of imagery [24].

H. Data Analysis

1) Analysis of Variance (ANOVA)

ANOVA is a statistical method used to compare two or more means under the assumption that the sampled populations are normally distributed. It is called ANOVA rather than a multi-group mean analysis, because it compares group means by analyzing comparisons of variance estimates. The difference between a t-test and ANOVA is that t-tests compares means to two groups and hence doing multiple two-sample t-tests would result in an increased chance of committing an error [25]. For this reason, ANOVAs are useful in comparing two, three or more means.

2) Linear Regression

A linear regression is a technique in which a straight line is fitted to a set of data points to measure the effect of a single independent variable [26]. The slope of the line is the measured impact of that variable. Simple linear regression involves discovering the equation for a line that most nearly fits the given data. That linear equation is then used to predict values for the data. A linear regression line has an equation of the form $\boldsymbol{Y = a + bX}$, where $\boldsymbol{X}$ is the explanatory variable and $\boldsymbol{Y}$ is the dependent variable. The slope of the line is $\boldsymbol{b}$, and $\boldsymbol{a}$ is the intercept (the value of $\boldsymbol{y}$ when $\boldsymbol{x} = 0$). A scatterplot can be a helpful tool in determining the strength of the relationship between two variables [27].

Correlation describes the strength, or degree, of linear relationship. That is, correlation allows specification to determine to what extent the two variables behave alike or vary together. Correlation analysis is used to assess the simultaneous variability of a collection of variables. [27]

III. METHODOLOGY

The data used for the research considered sea surface temperature measurements from two platforms; The Satellite data and insitu Buoy Data.

A. Satellite Data

The satellite data was obtained using the National Oceanic and Atmospheric Administration (NOAA) Polar Orbiting Satellites; NOAA-15, NOAA-16, NOAA-18 and NOAA-19. These datasets or measurements were obtained from the Center of Excellence in Remote Sensing Education and Research (CERSER) site (http:// cerser.ecsu.edu/terascan). The images available were available in the jpeg picture format. This data, due to its format lacked coordinate information as well as the actual temperature readings assigned to each pixel on the image. The image was however an RGB composite covering the coastline of North Carolina. The image also displayed a temperature legend or a color bar at the bottom, which estimated the temperature range within a given color index. Due to

these limitations, the SST's could not be measured by viewing actual digital number (DN) values. The satellite images obtained, covered the period from 22nd April, 2011 to 14th June, 2011. Within this period 101 images were selected for processing and finally compared to the insitu data. The images were also selected based on the amount of cloud cover present above the regions of interest within the image. It was thus ensured that the image selected had at least two of the three points to be considered in the image being free of cloud cover.

1) Visualization and SST Extraction

Before approximations of the SST's were made, a simple geo-referencing was applied to the image using the ILWIS image processing software. The buoy coordinates were imported into Google Earth and with this, ground control points were taken using visually distinct features within the designated area. The coordinate system was then introduced into the jpeg image by adding ground control points from the coordinates obtained in Google Earth. With a coordinate system placed on the image, the approximate pixel locations of the three buoys could be located on the image. The buoy pixel locations were then available and thus there was no further need to perform geo-referencing on the remaining images. The SST could then be measured for each buoy location by navigating to the identified pixel location for each of the specific buoys. This was done using the ENVI 4.7 imaging software due to its enhanced zooming options. The identified pixel would then be zoomed in to reveal its color and also avoided the surrounding pixels from saturating the particular pixel of interest. The color obtained from the desired pixel was then compared to the temperature legend of the image to give the approximated SST measurement in Degrees Celsius (oC). This step was then repeated in all the acquired images to produce the SST for all three points in all the images.

B. Buoy Data

Three buoys were used in the verification of the SST obtained from the satellite images. These were all located off the coast of North Carolina. The buoys were operated by The Center for Operational Oceanographic Products and Services (CO-OPS) of the National Ocean Service (NOS). The buoys are listed in FIGURE 1

Station DUKN7 – Duck Pier NC - 36.183N 75.747W
Station ORIN7 – Oregon Inlet Marina NC – 35.795N 75.548W
Station HCGN7 – Hatteras, NC - 35.208N 75.703W

Figure 1: Buoys and locations

The SST readings for the above mentioned buoys were retrieved from the National Data Buoy Center (http://ndbc.noaa.gov/). These readings were also taken from 22nd April 2011 to 14th June 2011, at approximately the same time as the satellite readings. Temperature records were done using the Coordinated Universal Time (UTC) to ensure that both readings were done within the same time zone. The Archived datasets were then copied into an excel sheet for comparison with the satellite SST. After both datasets were collected, they were then subjected to statistical analysis.

1) Statistical Data Analysis

The main tools used in the data analysis procedures included Microsoft Office Excel 2010 Spreadsheet software and Minitab 15. The first procedure involved an analysis of variance (ANOVA), which was carried out in Minitab 15. This stage applied the balanced ANOVA method. The satellite SST was used as the predictors while the buoy SST as the response. This was ran in all the various regions of interest where the SST's had been gathered. The confidence interval for the test was set at 95% based on the t-distribution. The formulated hypothesis would then be accepted or rejected based on the results from this test. The P-value from the test resulted in 0.001, which meant there was a statistically significant difference in the temperatures. With statistical proof that the variance was significant the next procedure involved conducting regression analysis on both datasets. This was done on an individual site basis in Microsoft Office Excel Spreadsheet software. Both SST datasets were then displayed as scatter plots, and a trendline was applied to the created chart. A regression analysis was then run to display the R^2 value on the chart, which represented the coefficient

of determination. Based on the results of the regression a model equation would be created if the compared datasets showed at least 50% correlation. With both regression and ANOVA implemented, the following issues could be addressed:

- Finding a statistical difference in the SST readings from the satellite and buoy at 5% level of significance
- Which satellite-buoy relationship had the highest correlation
- Which NOAA satellite produced the most accurate SST reading

IV. RESULTS

The time series plot of the two datasets showed the HCGN Buoy generally recorded higher SST as compared to the NOAA satellite AVHRR sensor as seen in FIGURE 2.

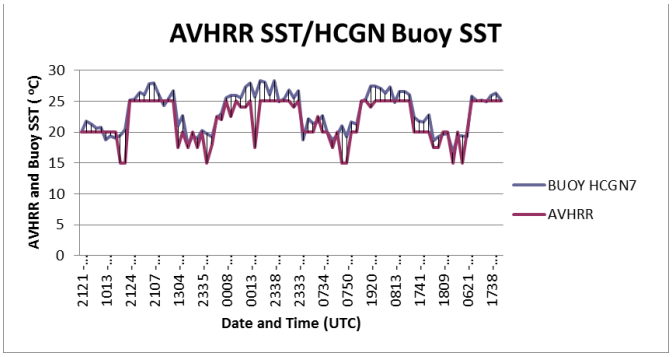

Figure 2: Time series plot of AVHRR SST and HCGN7 Buoy SST

The AVHRR/Buoy comparison revealed a mean temperature difference of +1.44 thus inferring that the buoy recorded an average temperature that was 1.44 degrees Celsius higher than that recorded by the AVHRR sensor.

Further analysis was carried out on the two groups of data by means of a linear regression analysis. This showed a correlation between the Buoy and the AVHRR sensor SST with an R^2 value of 0.75. Given that the regression showed correlation of more than 50% a model could be created for the difference in SST using the equation $Y = 0.8939x + 1.0254$ from FIGURE 3.

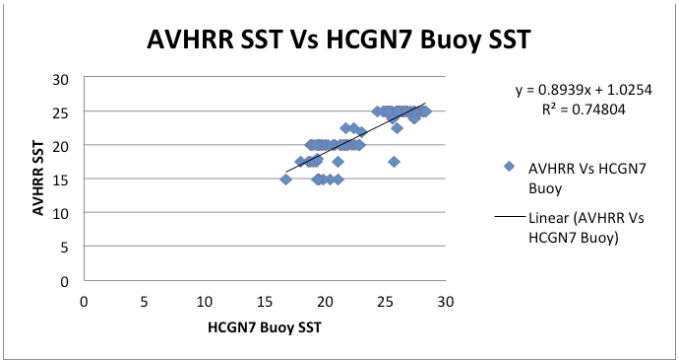

Figure 3: Linear regression analysis of AVHRR SST Vs. HCGN7 Buoy SST

The next comparison between the DUKN7 Buoy and its corresponding AVHRR SST measurements showed great variations in the measured SST of the two datasets as seen in figure 4.

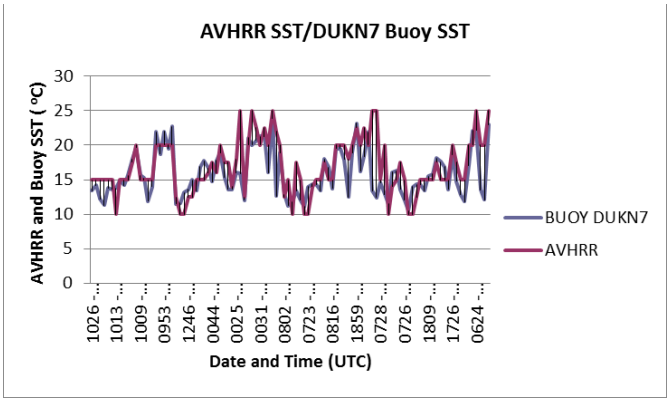

Figure 4: Time series plot of AVHRR SST and DUKN7 Buoy SST

A mean temperature difference of -1.11 degrees Celsius was observed between the Buoy and the AVHRR SST. This was the highest mean temperature difference recorded for all SST comparisons under this project. This implied that the AVHRR predicted temperatures were warmer than the Buoy SST by 1.11 degrees Celsius.

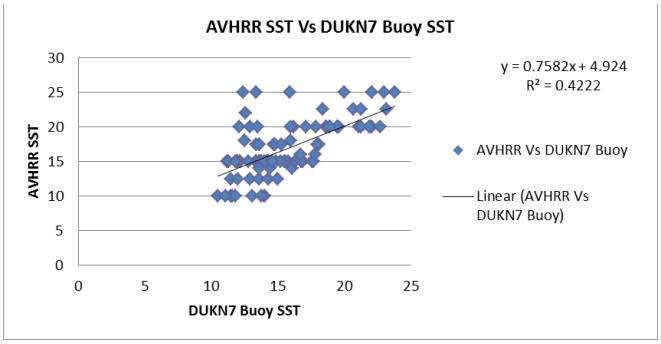

Figure 5: Linear regression analysis of AVHRR SST Vs. DUKN7 Buoy SST

Linear regression carried out on the same datasets (FIGURE 5) also revealed what was speculated when an R2 value of 0.42 was obtained. Since the correlation observed was less than the benchmark fifty percent (50%) stated by our objectives, the model ($Y = 0.7582x + 4.924$) for the AVHRR SST – DUKN7 Buoy relationship would not be a suitable or accurate correction formula.

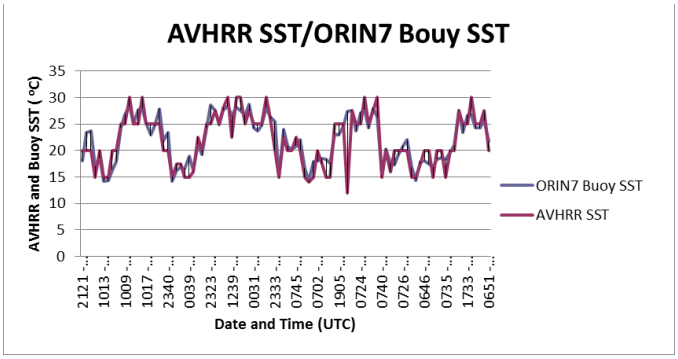

Figure 6: Time series plot of AVHRR SST and ORIN7 Buoy SST

From the time series plot displayed in FIGURE 6 the AVHRR SST was observed to be slightly lower than the SST measurements made by the ORIN7Buoy. A mean difference of +0.27 degrees Celsius was observed inferring that the ORIN7 Buoy SST measurements were slightly higher than the AVHRR SST on the average. This also implied that this data set had the least variance since it recorded the least mean SST difference among all the comparisons.

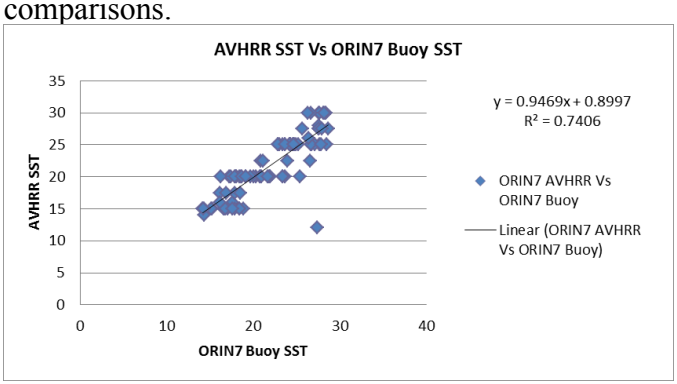

Figure 7: Linear regression analysis of AVHRR SST Vs. ORIN7 Buoy SST

The linear regression carried out for the AVHRR –ORIN7 Buoy SST in figure 7, recorded an R^2 value of 0.74 implying a good correlation between the two measurements. With a correlation of 74%, the model, $\boldsymbol{Y = 0.9469x + 0.8997}$ could be used in modeling AVHRR SST measurements with more accuracy with respect to the ORIN7 Buoy.

Because the AVHRR SST measurements came from different sensors (NOAA-15, NOAA-16, NOAA-18 and NOAA-19), it was necessary to compare SST measurements between each sensor. The goal was to determine if one sensor was more accurate than the other as shown in figure 8

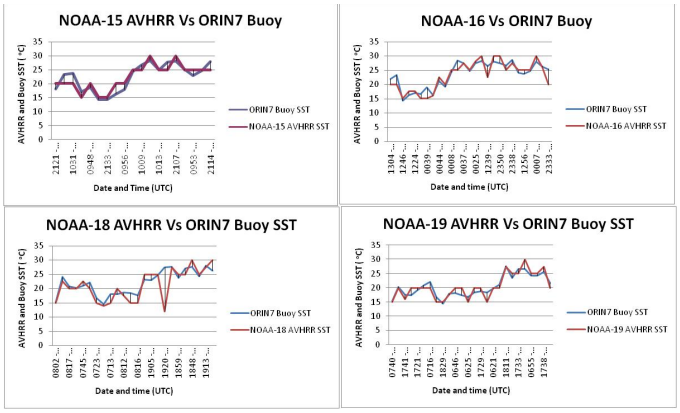

Figure 8: Time series plot of all NOAA AVHRR SST Vs ORIN7 Buoy SST

On the average, the NOAA-18 AVHRR sensor recorded the highest variance when compared to the Buoy SST. The mean temperature difference observed for this comparison was 0.770833 degrees Celsius. The lowest mean temperature difference was measured by the NOAA-15 AVHRR sensor recording an average temperature difference of -0.02105 degrees Celsius between buoy and the sensor. This implied that on the average NOAA-15 AVHRR SST were slightly higher than the temperatures recorded off the ORIN7 Buoy. The NOAA-16 and NOAA-19 sensors recorded mean temperature differences of 0.414815 and -0.11923 respectively.

With respect to the linear regression analysis carried out on all NOAA AVHRR SST sensors, correlations were drawn between the satellite sensors and the ORIN7 Buoy. The highest correlation was observed between the NOAA-16 AVHRR sensors and the Buoy SST measurements. The calculated coefficient of determination for this comparison was the highest for this comparison at 0.858. The NOAA-19 and NOAA-15 AVHRR sensors also recorded high correlations with the buoy with calculated R2 values of 0.840 and 0.801 respectively. In this light the most appropriate AVHRR sensor to use in SST comparisons or estimations based on the ORIN7 Buoy would be the NOAA-16 AVHRR. A model for

the correction of the AVHRR SST can then be employed by making use of the equation $Y = 1.002x - 0.289$.

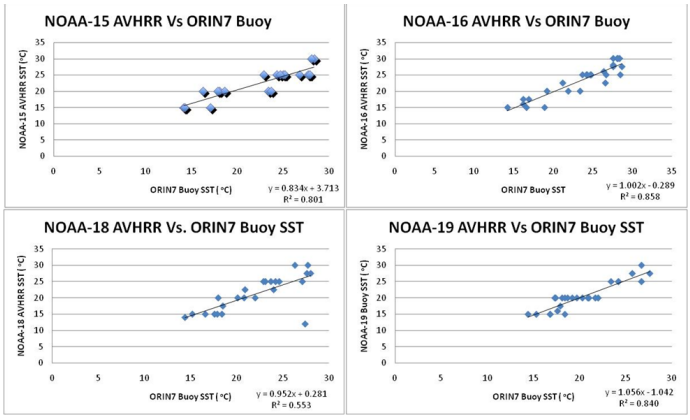

Figure 9: Linear regression analysis of all NOAA AVHRR SST Vs ORIN7 Buoy SST

V. CONCLUSION

In conclusion, it was observed that there was a statistical difference between the buoy and satellite measurements at a 95% level of confidence for all the sites.

Based on the results of the project it could be deduced that the NOAA AVHRR SST measurements were comparable to the SST of the HCGN and ORIN7 buoy with the ORIN7 buoy comparison being the most consistent with an R^2 value of 0.74 and mean temperature difference of $+0.27^{o}$C. A further comparison of the all the NOAA AVHRR sensors saw the NOAA-16 AVHRR emerging as the most consistent with the ORIN7 buoy data by having the highest correlation of 0.855 when compared with the Buoy SST measurements over the same period.

VI. FUTURE WORK

Results from this project infer that while comparable by most standards, AVHRR SST measurements still needed improvements. The readings can be improved in future studies by using the correct data formats for the NOAA-AVHRR images. This can be obtained by processing raw or level 0 data using the appropriate channels in TeraScan to derive the SST product. This discovery also led to the creation of master files to derive products for specific areas of interest. This is useful in saving time and space during the processing periods. The Terascan training obtained during the period also revealed that the jpeg format was not an ideal image format for the project that was carried out. The derived products should thus be stored as a geotiffs, HDF or NETCDF to retain the data as well as coordinate information, which are of key interest. This can then be exported to other third party software for use in future comparisons while maintaining the actual data. For purposes of display on the server, the Jpeg and Geotiff formats may be used with links to download sites for the HDF and NETCDF formats for more detailed information.

Because there was a tendency for the AVHRR SST measurements to undervalue the observed SST, a comparison needs to be made between AVHRR SST and additional atmospheric variables such as wind speed, air temperature, and humidity. This can be done to investigate if any of these variables will affect the performance of the AVHRR sensor. In a study described by Malrig in 2009, his study revealed a relationship between humidity and the performance of AVHRR SST temperatures.

ACKNOWLEDGMENT

Our sincerest gratitude goes to Dr. Linda Hayden for making the research opportunity in Ocean, Marine, and Polar Sciences available to us as well as providing the means for us to get to the country. We would also like to thank who Dr. George Wiafe (University of Ghana) for introducing and nominating us for the URE OMPS. Special thanks to our mentors Mr. Je'aime Powell and Mr. Kuchumbi Hayden for their great mentorship.

REFERENCES

[1] Lillesand, Thomas M., Ralph W. Kiefer, and Jonathan W. Chipman2004 Remote Sensing and Image Interpretation, Fifth edition. Wiley, New York.

[2] Schott, John Robert (2007). Remote sensing: The image chain approach (2nd ed.). Oxford University Press.p.1.ISBN9780195178173.

[3] Liu, JianGuo& Mason, Philippa J. (2009). Essential Image Processing for GIS and Remote Sensing. Wiley-Blackwell. p. 4. ISBN 978-0-470-51032-2

[4] "Ground Truth; The "Multi" Concept; Imaging Spectroscopy"[Online] Available: http://rst.gsfc.nasa.gov/Sect13/Sect13_1.html

[5] "Groundstations." [online] (2010) Available: http://www.seaspace.com/?mid=groundstations Accessed 30th June 2011.

[6] "What is Terascan." [online] (2010) Available: http://psbcw1.nesdis.noaa.gov/terascan/home_basic/what_is_terascan.html#Satellites Accessed 30th June 2011.

[7] Turner, D.B. (1994). Workbook of atmospheric dispersion estimates: an introduction to dispersion modeling (2nd Edition ed.). CRC Press. ISBN 1-56670-023-X. CRCpress.com)

[8] Beychok, M.R. (2005). Fundamentals Of Stack Gas Dispersion (4th Edition ed.).author-published. ISBN 0-9644588-0-2.www.air-dispersion.com

[9] Pearce, Fred, The Climate Files: The Battle for the Truth about Global Warming, (2010) Guardian Books, ISBN: 978-0-85265-229-9, p. XVIII.

[10] "Polar-Orbiting Satellites" [Online]. Available: http://psbcw1.nesdis.noaa.gov/terascan/home_basic/polar_sats_overview.htm Accessed: 6th July, 2011.

[11] "Constellation of L-band/S-band Polar-Orbiting Satellites" [Online]. Available: http://psbcw1.nesdis.noaa.gov/terascan/home_basic/polar_sats_overview.htm. Accessed: 6th July, 2011

[12] Sensors of Polar-Orbiting Satellites. [Online]. Available: http://psbcw1.nesdis.noaa.gov/terascan/home_basic/polarsats_sensors_tables.html#AVHRR. Accessed: 6th July, 2011

[13] Malvig S., 2009: Comparison of Observed Sea Surface Temperatures vs. Advanced Very High Resolution Radiometer (AVHRR) Sea Surface Temperatures OC/MR 3570 - PROJECT

[14] "Sea Surface Temperature Product" [Online]. Available: (http://saf.met.no/p/sst/index.html) Accessed: 12th July 2011.

[15] Reusch, William (1999). "Infrared Spectroscopy". Michigan State University. Retrieved 2006-10-27).

[16] Dr. S. C. Liew. "Electromagnetic Waves". Centre for Remote Imaging, Sensing and Processing. Retrieved 2006-10-27.

[17] Goldsmith, JR (December 1997). "Epidemiologic evidence relevant to radar (microwave) effects".Environmental Health Perspectives105 (Suppl. 6): 1579–1587)

[18] Liou, Kuo-Nan (2002). An introduction to atmospheric radiation. Academic Press. p. 2. ISBN 0124514510. Retrieved 12 July 2010)

[19] "ILWIS GIS/Remote Sensing Software." [Online] Available: http://www.ilwis.org/index.htm Accessed: 6th July 2011.

[20] "ILWIS - Remote Sensing and GIS software." [Online] Available: http://www.itc.nl/Pub/Home/Research/Research_output/ILWIS_-_Remote_Sensing_and_GIS_software.html. Accessed: 6th July 2011.

[21] "GEONETCast Toolbox Software." [Online] Available: http://52north.org/communities/earth-observation/geonetcast-toolbox-software

[22] "ITC GEONETCast Toolbox." [Online] (2011) Available: http://www.itc.nl/Pub/Organization/Geonetcast-Toolbox.html Accessed: 6th July 2011.

[23] "The Basics of ENVI and the Nature of Digital Images" [Online] Available: http://geography.tamu.edu/class/aklein/geog361/lab_exercises/lab01_instructions.pdf Accessed 6th July, 2011.

[24] "ENVI Capabilities." [Online] Available:http://www.ittvis.com/language/en-us/productsservices/envi/capabilities.aspx. Accessed: 6th July 2011

[25] "Analysis of Variance." [Online]. Available: http://www.sjsu.edu/faculty/gerstman/StatPrimer/anova-a.pdf. Accessed: 6th July 2011.

[26] Linear Regression: [Online]. Available: http://www.investorwords.com/2829/linear_regression.html#ixzz1SMvUsztS. Accessed on 16th July 2011.

[27] Linear Regression [Online]. Available:http://www.stat.yale.edu/Courses/1997-98/101/linreg.htm Accessed on 16th July 2011.